Heat Transfer Analysis of a Gas-Jet
Laser Chemical Vapor Deposition (LCVD) Process

Chad E. Duty, Brian T. Fuhrman, Daniel L. Jean, and W. Jack Lackey
Rapid Prototyping and Manufacturing Institute
Woodruff School of Mechanical Engineering
Georgia Institute of Technology
Atlanta, GA 30332

Abstract

This paper describes the development of a computer model used to characterize the heat transfer properties of a gas-jet LCVD process. A commercial software package was used to combine heat transfer finite element analysis with the capabilities of computational fluid dynamic software (CFDS). Such a model is able to account for both conduction and forced convection modes of heat transfer. The maximum substrate temperature was studied as a function of laser power and gas-jet velocity.

Introduction

Laser chemical vapor deposition (LCVD) is a relatively new manufacturing process that holds great potential for the production of small and complex metallic and ceramic parts. A sophisticated gas-jet LCVD system has been designed and developed at Georgia Tech. The system promises increased geometric flexibility and deposition rates and is designed to function as a rapid prototyping system. The system is currently under development to understand and optimize key processing parameters. Since CVD is a thermally activated process, the most important process variable is temperature. In a laser-heated process such as pyrolytic LCVD, the temperature field is restricted to a micron scale and can vary by an order of magnitude over the diameter of the laser spot. Deposition rates typically follow an Arrhenius relationship that is exponential with respect to temperature, so it is critical to document and understand these two-dimensional temperature variations.

Background

A number of theoretical and experimental studies have attempted to model and understand the role of temperature in the LCVD process. Before the advent of LCVD, Kokorowski *et al.*[1] predicted temperature distributions in a substrate during continuous wave laser annealing. Conduction was the only mode of heat transfer considered, but he did account for temperature dependent material properties. Many studies[2-4] followed in the next 50 years, but few of the models allowed for forced flow convection and many did not account for temperature-dependent material properties.

Steen's[5] numerical model, developed in 1977, demonstrated that convection and radiant surface losses were significant in a temperature sensitive process. He introduced convection losses into the model by including a non-reacting gas jet that was coaxial with the laser beam. By restricting the jet to be coaxial, he preserved the axial symmetry of his model, making analytical calculations possible. Steen studied the thermal history of the substrate surface with respect to various process parameters, including the jet Reynolds number, the distance between the substrate and the nozzle mouth, the jet temperature, and the surface reflectivity.

In 1989, Mazumder and Kar[6] introduced a three-dimensional model that incorporated all three mechanisms of heat transfer (conduction, convection, and radiation). The analysis employed a technique of uniformly moving finite slabs to synthesize a moving laser beam at a constant velocity. In contrast to the previous infinite and semi-infinite geometric models, this analysis was much more applicable to smaller substrates whose overall dimensions were on the order of the laser spot diameter.

In 1998, Yu and Duncan[7] proposed a three-dimensional finite element model that was able to account for the natural convection fluid flow that results from laser heating. The model included conduction, convection, and radiation heat transfer mechanisms. A buoyancy-driven flow was determined by the Boussinesq principle and demonstrated during the horizontal growth of a fiber. Yu and Duncan assumed incompressible fluid, laminar flow, and steady state conditions. The effects of the natural convection were demonstrated in terms of temperature gradients and associated growth rates.

It is apparent that a significant amount of work has been performed in the area of LCVD process and thermal modeling. The analytical models and numerical analyses have progressed considerably over the years, however none of the models allow for a forced directional gas flow.

Model Development

## *Physical System Description*

Georgia Tech's gas-jet LCVD system is designed to optimize each aspect of the LCVD process with respect to build time, accuracy, resolution, and flexibility. The system has been described in detail in previous papers[8,9] and is shown schematically in Figure 1. A small reaction chamber houses a substrate on top of a moving and rotating shaft. High resolution, three-dimensional patterns can be created by numerically controlling the movement of the rotating stage assembly. By travelling in a spiral pattern, fast scanning speeds can be achieved without the high reversal forces typical of raster scanning. Reagent gases are introduced into the reaction chamber via a small diameter gas jet that impinges on the substrate at a 45° angle. The high-velocity jet generates a thin boundary layer for the diffusion of reagent gases, theoretically enhancing the chemical kinetics of the reaction and increasing the deposition rate. A carbon dioxide laser heats a spot on the substrate above the threshold temperature required to initiate pyrolytic LCVD reactions. The laser has a maximum power rating of 100 W and is focused to a beam diameter of 200 µm.
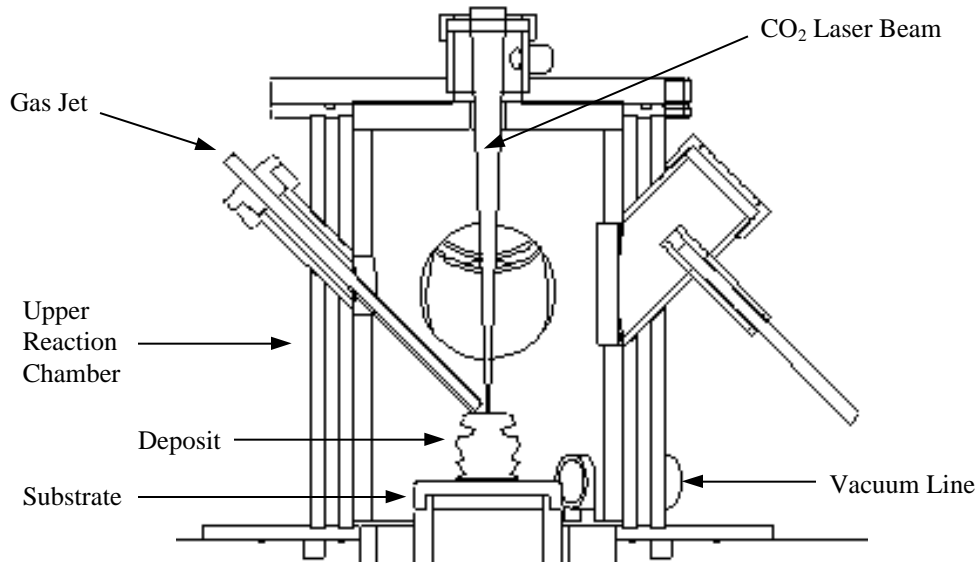
Figure 1. Cross Section View of LCVD Reaction Chamber

Model Geometry and Boundary Conditions

The reaction chamber geometry has been simplified in the finite element model in order to make calculations more efficient. Since the model is symmetric about the axis of the reagent jet, only one half of the area surrounding the gas-jet and laser spot is represented. The geometry and boundary conditions of the wedge-shaped model are illustrated in Figure 2. The substrate consists of a _ inch thick piece of graphite. A thin-walled tube geometry is suspended in the argon atmosphere above the substrate to represent the reagent gas-jet. The end of the tube is separated from the center of the laser spot by 3/16 of an inch. The laser spot is represented as a
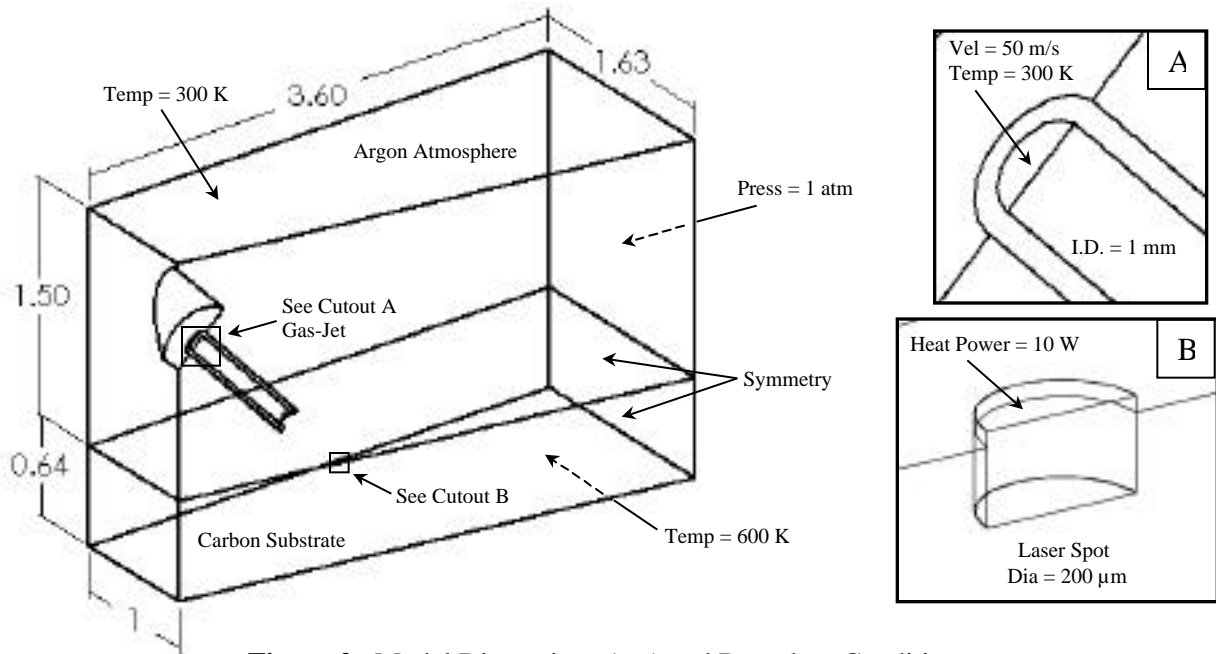

Figure 2. Model Dimensions (cm) and Boundary Conditions

small cylinder embedded in the carbon substrate. The cylinder protrudes from the substrate by 20 nm, simulating the first stages of deposit growth. This also allows for a complementary face within the argon atmosphere to be used to specify boundary conditions.

The physical properties of the laser cylinder and the carbon substrate are specified as grade ATJ isomolded graphite. The properties of the graphite and the argon are modeled as constant with respect to temperature. The fluid flow properties of the model are specified at a single inlet and outlet. Argon enters the tube with a specified velocity and temperature (see cutout 2-A). A typical inlet velocity used in practice is 50 m/s. The outlet is represented by a total pressure boundary of 1 atmosphere on the back face of the argon atmosphere. The laser power is represented as heat power boundary condition across the top face of the laser cylinder (see cutout 2-B). Since the heat power is applied to only one-half of the laser spot, the effective laser power is twice this amount (i.e. 10 W of applied heat power translates to a laser power of 20 W, assuming that the substrate is a blackbody). Physically, the laser in the LCVD process has a Gaussian distribution, but it is restricted in this model to a flat distribution. Constant temperature conditions were also set on the top and bottom surfaces of the model to respectively simulate room temperature (300 K) and the resistive heating element (600 K).

Figure 3 shows the result of the automatic meshing routine used by Cosmos/Works®. Mesh control conditions were set on the symmetry face of the laser cylinder and the terminating face of the gas-jet tube. The grid spacing on the laser face was restricted to 20 µm with a geometric growth rate of 1.15 over 25 layers. The grid spacing on the tube face was restricted to 100 µm with a geometric growth rate of 1.15 over 25 layers. These conditions resulted in a very fine mesh in the regions of interest while limiting the overall model to just under 16,000 nodes.
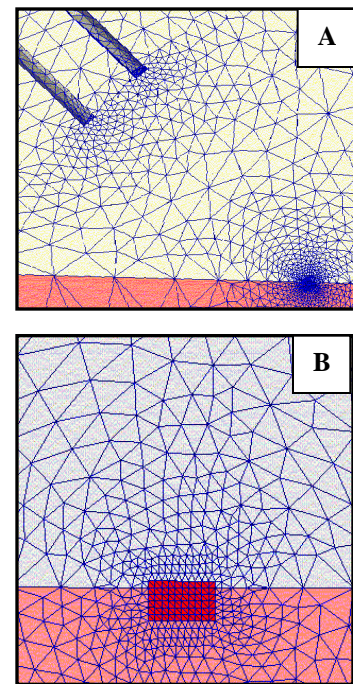
Figure 3. Mesh spacing on symmetry face for (a) tube and laser and (b) close-up of laser cylinder.

Model Evaluation and Results

The model was evaluated using a commercial code, Cosmos/Flow®, that is designed to solve the mathematical equations that represent heat transfer and momentum transfer in a moving fluid. The current model represents an initial phase in the development of a more sophisticated thermal model of the LVCD process. In this preliminary phase, conduction and forced convection will be the only modes of heat transfer considered. The effects of radiation and natural convection (buoyancy-driven flow) will be ignored. The internal flow is considered turbulent and fully compressible.

Figure 4 illustrates the flow velocity along the symmetry plane for an inlet velocity of 50 m/s. The laser spot is visible within the substrate and there appears to be significant flow just above the surface of the laser spot. Figure 5 shows how the temperature in this plane is affected by the gas-jet with no effects from the laser beam. The dominant mode of heat transfer around the laser spot is apparently conduction, since the surface temperature of the substrate is equal to the heater temperature of 600 K. Figure 6 is a contour plot of the gas flow just above the surface of the substrate (separation distance of ~100 µm). The location of the laser spot is shown as a white circle. Figure 7 demonstrates how the temperature within the laser spot varies when the laser power is 20 W and there is no argon flow in the chamber. The maximum temperature in this case is about 1700 K. Since the isotherms are not concentric circles, the symmetry conditions of the model may not be appropriately defined.
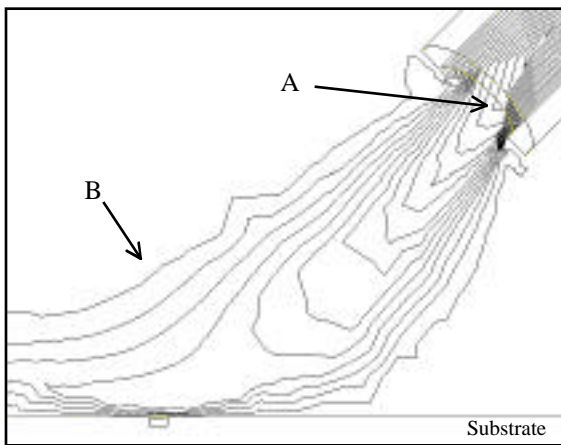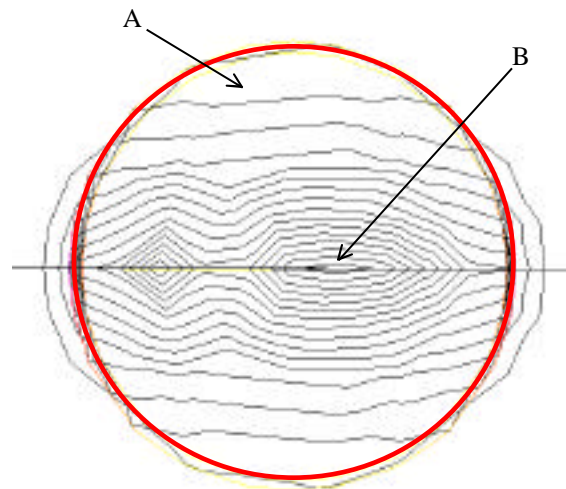

Figure 4. Flow Contours of Symmetry Plane. Inlet Velocity = 50 m/s.
$Vel_A = 35$ m/s $Vel_B = 0$ m/s
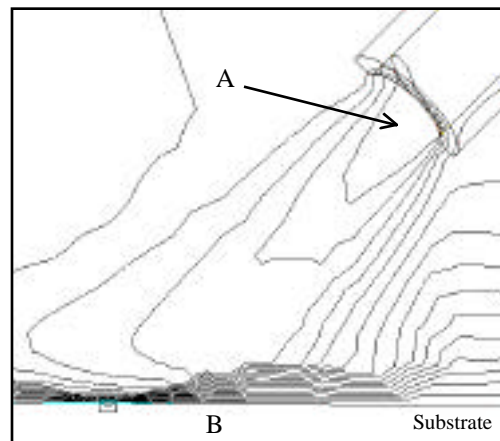
Figure 5. Temperature Contours of Symmetry Plane. Power = 0 W, Vel = 50 m/s.
$T_A = 300$ K $T_B = 600$ K
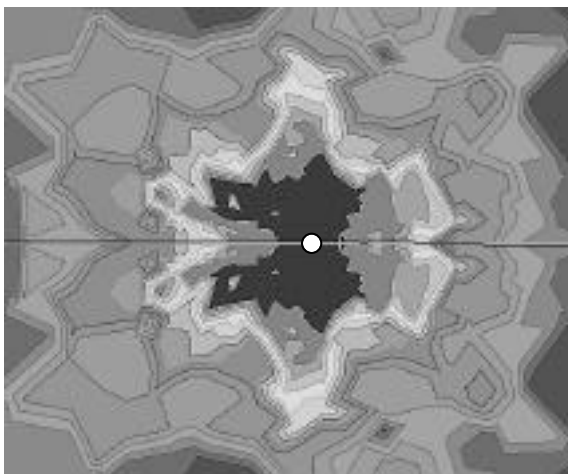
Figure 6. Flow Contours above Laser Spot. Inlet Velocity = 50 m/s.
Center Vel = 10 m/s   Edge Vel = 0 m/s

Figure 7. Temperature Contours of Laser Spot. Power = 20 W, Vel = 0 m/s.
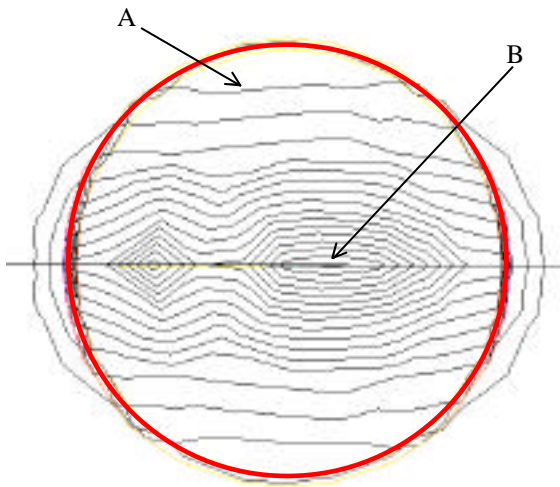$T_A = 900$ K $T_B = 1680$ K

Figures 8 through 10 below show temperature variations across the laser spot at several values for the inlet flow velocity. In each case, fluid flow is from the right and the laser power is constant at 20 W. The resulting plots are nearly identical, both in terms of absolute temperatures and distributions. Surprisingly, this suggests that convection heat transfer plays an insignificant role in the LCVD process. Another interesting feature is the existence of two distinct hot pockets along the centerline of each spot. The cause of these is unclear, though it can most likely be attributed to ill-defined symmetry conditions of the model.
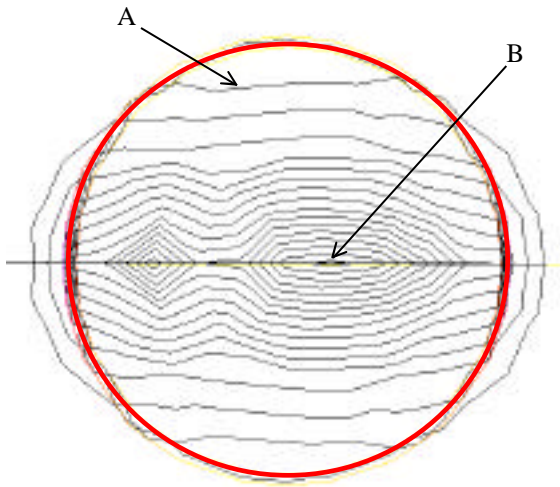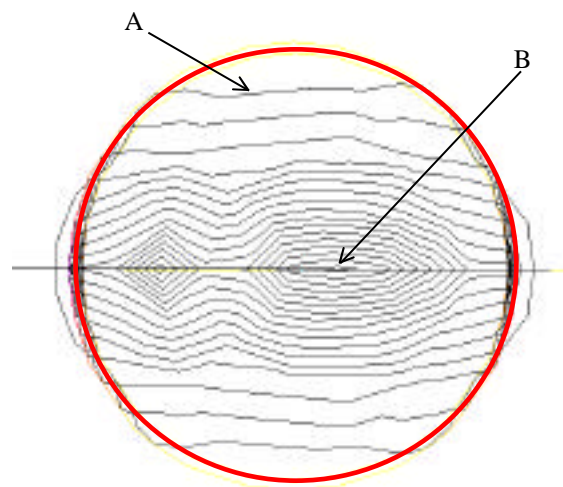
Figure 8. Temperature Contours of Laser Spot. Power = 20 W, Vel = 30 m/s. T_A = 900 K T_B = 1700 K
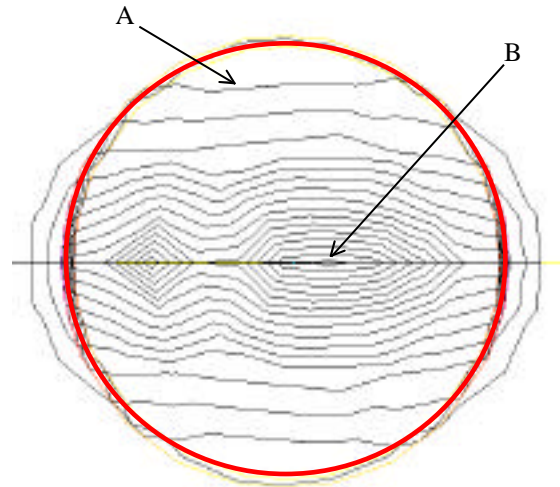
Figure 9. Temperature Contours of Laser Spot. Power = 20 W, Vel = 50 m/s. T_A = 900 K T_B = 1700 K

Figure 10. Temperature Contours of Laser Spot. Power = 20 W, Vel = 100 m/s. T_A = 900 K T_B = 1700 K

Figure 11. Temperature Contours of Laser Spot. Power = 80 W, Vel = 50 m/s. T_A = 2000 K T_B = 5000 K

Figure 11 on the previous page illustrates typical temperature variations at higher laser powers. Although the absolute temperatures are higher, the relative distribution across the laser spot is nearly identical to those with lower laser powers. Figure 12 plots the maximum temperature within the laser spot for a range of laser powers. The result of elevating the substrate temperature by increasing the laser power is hardly unexpected. The surprising outcome is the linear correlation of the data -- it is perfectly linear with an intercept of 600 K and a slope of 56 K/W.
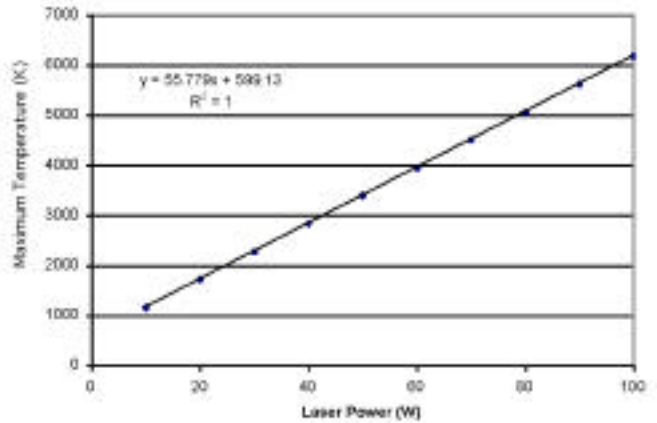

Figure 12. Temperature vs. Laser Power

Discussion

The results suggest that the gas flow velocity has a negligible effect on the absolute temperature and temperature distribution within the laser spot. Therefore, it appears that convection is not a significant mode of heat transfer under the conditions of this model. This result is unexpected considering the proximity of a high velocity gas-jet. However, a quick analysis shows that the energy absorbed by the passing argon gas per unit time is about 1% of the power supplied by the laser.

Consider that argon is flowing out of the nozzle at 50 m/s. Given the diameter of the nozzle and a density for argon of 0.5 kg/m^3, the mass flow out of the gas-jet is 4E-05 kg/s. Suppose that as the jet expands and approaches the 200 µm laser spot, about 1% of the gas passes directly over that area. From the results of the above model (Figure 9), we see that the maximum temperature across the laser spot is about 1700 K for a laser power of 20 W. Given that the heat capacity of argon is 520 J / kg / K and the original substrate temperature is 600 K, it is possible to calculate the energy absorbed by the argon gas as it passes over the laser spot.

$$P = \Delta T \ (dm/dt) \ c_p = (1700 - 600 \ K) \ (4E\text{-}07 \ kg/m^3) \ (520 \ J/kg/K) = 0.23 \ J/s = 1.1 \ \% \ of \ 20 \ W$$

This is a rough estimate, but it supports the idea that convection is not a dominant mode of heat transfer under these conditions. The linear behavior of Figure 12 can be interpreted more appropriately once conduction is identified as the sole source of heat transfer (remember that radiation is not included in this model). Conservation of energy requires that the heat flux generated by the laser must equal the heat flux dissipated by conduction. This is expressed below along with the basic form of the conduction equation. The terms for conductivity and area remain constant with respect to temperature in this model. Therefore, the conductivity equation can be rearranged into the linear y = m x + b format as shown below. With this perspective, the linear relationship of Figure 12 is not so surprising -- it merely points to a conduction-dominated process. Furthermore, the y-intercept equals the original substrate temperature, 600 K.

467

$$\text{flux}_{\text{laser}} \; = \; \text{flux}_{\text{conduct}} = \; k / A \; (\; T \;) \quad \blacktriangleright \quad T_{\text{max}} = \; (A / k) \, \text{flux} \; + \; T_o$$

Conclusions

LCVD is a process dominated by temperature. It is imperative to study and accurately model the temperature variations in and around the laser spot. The current model provides a rough estimate and serves as an important first step in the development of a more accurate model. A surprising conclusion from this model is the relatively small impact of convection on the heat transfer of the gas-jet LCVD process. We will attempt to verify this result through future versions of the model that will include temperature-dependant material properties, natural convection, radiation, and a Gaussian beam distribution. One should hesitate, however, to discount convection as a possible source of heat transfer based on this model alone.

Acknowledgements

References

1. S.A. Kokorowski, G.L. Olson, and L.D. Hess. *Proceedings of Laser and Electron-Beam Solid Interactions and Material Processing.* J.F. Gibbons, L.D. Hess, and T.W. Sigmon, eds. New York 1955. pp. 139-146.

2. J.E. Moody and R.H. Hendel. "Temperature Profiles Induced by a Scanning cw Laser Beam." *Journal of Applied Physics* **53.** 1982. p. 4364.

3. T.T. Rantala and J. Levoska. "A Numerical Simulation for the Laser-Induced Temperature Distribution." *Journal of Applied Physics* **65** (12). 1989. pp. 4475-4479.

4. J. Han and K. Jensen. "Combined Experimental and Modeling Studies of Laser-Assisted CVD of Cu from Copper(l)-Hexafluoroacetylacetonate Trimethylvinylsilane." *Journal of Applied Physics* **75** (4). 1994. pp. 2240-2250.

5. W.M. Steen. "The Thermal History of a Spot Heated by a Laser." *Letters in Heat and Mass Transfer* **4.** 1977. p. 167.

6. J. Mazumder and A. Kar. *Theory and Application of Laser Chemical Vapor Deposition.* Plenum Press, New York. 1995. pp. 215-293.

7. D. Yu and A. Duncan. "Investigation of Induced Thermal and Fluid Transport Phenomena in Laser Assisted Chemical Vapor Deposition." *Proceedings of the ASME Heat Transfer Division* **361** (4). 1998. pp. 183-191.

8. C. Duty, D. Jean, and W.J. Lackey. "Laser CVD Rapid Prototyping." *Proceedings of The American Ceramic Society Meeting* Cocoa Beach, Florida. Jan 1999. pp. 347-354.

9. D. Jean, C. Duty, B. Fuhrman, and W.J. Lackey. "Precision LCVD System Design with Real Time Process Control." *Proceedings Solid Freeform Fabrication Symposium* Austin, Texas. August 1999. pp. 59-65.